SYNTHESIS AND CHARACTERIZATION OF METAL OXIDE NANOPARTICLES FOR REFINERY APPLICATIONS

Project Report

Submitted by:

KULDEEP SINGH
(R670215021)

in partial fulfillment for the award

of the degree of

MASTER OF TECHNOLOGY

IN

Chemical Engineering with Specialization in Process Design Engineering

Under the guidance of:

Dr. Harender Bisht
Group Lead Coking Technology,
Refining R&D,
Reliance Industries Ltd.
Jamnagar

Dr. R. Mahajan
Associate Professor
Department of Chemical Engineering
University of Petroleum and Energy Studies
Dehradun

APRIL - 2017

CERTIFICATE

This is to certify that the thesis titled "**SYNTHESIS AND CHARACTERIZATION OF METAL OXIDE NANOPARTICLES FOR REFINERY APPLICATIONS**" submitted by **KULDEEP SINGH (R670215021)**, to the University of Petroleum & Energy Studies, for the award of the degree of **MASTER OF TECHNOLOGY** in Chemical Engineering with specialization in Process Design Engineering is a bonafide record of project work carried out by him under our supervision and guidance. The content of the thesis, in full or parts have not been submitted to any other Institute or University for the award of any other degree or diploma.

Guided By:
Dr. Harender Bisht
Group Lead Coking Technology,
Refining R&D
Jamnagar, Gujarat - 361142

Guided By:
Dr. R. Mahajan
UPES
Deptt of Chemical Engineering
Dehradun - 248007

Signature of Head of the Department

Date: _____

ACKNOWLEDGEMENTS

I am grateful to the Dr. Asit K. Das, HOD, Refining R&D, Reliance industries Ltd for extending the opportunity of internship at RIL. His supervision, guidance and motivation is highly encouraging for me.

I would like to express my gratitude to my guide, Dr. Harender Bisht, whose expertise, understanding, generous guidance and support made it possible for me to work on a topic that was different and new for me. It is a great pleasure and great learning experience to work with you.

I am hugely indebted to Dr. R. Mahajan, my internal guide and my professor, for finding out time to reply to my e-mails, for being ever so kind to show interest in my research and for giving his precious and kind advice regarding the topic of my research.

I am grateful to Mr. Ashwani Yadav & Mr. Dwaipayan Biswas for helping me out with the lab procedures and equipment. Your constant support and guidance was crucial to the completion of the thesis.

I am also obliged to Dr. Vijay Balachandran at RCP for providing me DLS & TEM analysis in my project.

I want to thank Mr. Gopinath Sir, my course coordinator for all the help and support in smooth functioning of our internship and it's concerning proceedings. His advice and guidelines have been helpful during the past eight months.

I would like to express my sincere gratitude to all those people who have directly or indirectly contributed to the completion of this thesis. Without your support, it would not have been possible to complete this project.

ABSTRACT

Nanotechnology refers to manipulating and controlling the arrangement of atoms in the range of few nanometers typically from 1nm to 100nm. Nanotechnology has the potential to create many new materials and devices with wide ranging applications, such as in medicine for drug delivery, in electronics using silica nano-coating to make water proof mobiles, in energy production using quantum dot coated solar cells and also in the fields of refining and processing.

Today, a range of elements and compounds not only synthesized and characterized in nanometer-scale but they have been successfully deployed as commercial products e.g., metals & metal oxide nanoparticles, nanoscale semiconductors, Carbon nanotubes, Graphene etc. Nanotechnology has also found several important applications in refining and petrochemical industry such as nano-adsorbents and nano-catalysts.

This report covers literature survey of Cerium oxide, Bismuth oxide, Magnesium oxide, Zirconium oxide, Antimony oxide, Iron oxide, Copper oxide, Molybdenum oxide & Zinc oxide nanoparticles (MONs). It includes synthesis and characterization of Cerium oxide, magnesium oxide & bismuth oxide nanoparticles in aqueous medium and their transfer to hydrocarbon medium to form stable dispersion.

Keywords: Metal oxide nanoparticles; MONs; CeO_2; MgO; Bi_2O_3; ZrO_2; TiO2; ZnO; Fe_3O_4; SnO; CuO; structural and electronic properties; physico-chemical properties; nanostructure.

TABLE OF CONTENTS

CHAPTER 1 INTRODUCTION ……..... 1

1.1 Basics of Nanotechnology.……1

1.2 Applications of nanotechnology
in the field of refining and processing.…… 2

CHAPTER 2 LITERATURE REVIEW ……..…… 3

2.1 Nanoparticles and Nano-scale materials……..…… …… 3

2.2 Synthesis techniques for Nano particles…… 4

2.2.1 Co-precipitation method……..…… 5

2.2.2 Colloidal method……..……6

2.2.3 Sol-gel method……..…… 6

2.2.4 Micro- emulsion technique……..…….7

2.3 Characterization techniques for Nano particles……..……..8

2.3.1 Scanning electron microscope (SEM)……..….9

2.3.2 Transmission electron microscope (TEM)…… 11

2.3.3 X-Ray Diffraction (XRD)…… 13

2.3.4 Dynamic Light Scattering (DLS)…….. 14

2.4 Synthesis and characterization of Metal oxide
Nanoparticles……..... 16

2.4.1 Background…… . …….. 16

2.4.2 Iron oxide…… …….. 16

2.4.3 Zinc oxide……..…… 18

2.4.4 Copper oxide……..…… 19

2.4.5 Bismuth oxide……..... .. 20

2.4.6 Antimony oxide…… . 21

2.4.7 Magnesium oxide……....… 22

2.4.8 Cerium oxide……..... 24
2.4.9 Zirconium oxide……..…... 26
2.4.10 Molybdenum oxide……..... . 27
2.5 Stabilization of metal oxide nanoparticles…….....28
2.5.1 Aqueous phase to hydrocarbon phase transfer…….28
2.5.2 Mechanism of stabilization…….....29
2.5.3 HLB of various surfactants……..…… 29

CHAPTER 3 MATERIAL AND METHODOLOGY……. 32

3.1 Synthesis of MgO nanoparticles……..…….....39
3.2 Synthesis of CeO_2 nanoparticles……45
3.3 Synthesis of Bi_2O_3 nanoparticles……...51

CHAPTER 4 RESULT AND DISCUSSION……..…. 56
CHAPTER 5 CONCLUSION……..

REFERENCES……..…....58

LIST OF TABLES

TABLE 2.1. HLB OF VARIOUS STABILIZERS……35

TABLE. 3.1. EXPERIMENTAL DETAILS OF MgO NANOPARTICLES……37

TABLE. 3.2. AMOUNT OF STABILIZER NEEDED TO STABILIZE MgO NANOPARTICLES……38

TABLE. 3.3. STOCK SOLUTION FOR DLS ANALYSIS OF MgO NANOPARTICLES……40

TABLE. 3.4. AVERAGE DIAMETER OF MgO NANOPARTICLES WITH DIFFERENT STABILIZERS……40

TABLE. 3.5. EXPERIMENTAL DETAILS OF CeO_2 NANOPARTICLES……43

TABLE. 3.6. AMOUNT OF STABILIZER NEEDED TO STABILIZE CeO_2 NANOPARTICLES……45

TABLE. 3.7. STOCK SOLUTION FOR DLS ANALYSIS OF CeO_2 NANOPARTICLES……46

TABLE. 3.8. AVERAGE DIAMETER OF CeO_2 NANOPARTICLES WITH DIFFERENT STABILIZERS……46

TABLE. 3.9. EXPERIMENTAL DETAILS OF Bi_2O_3 NANOPARTICLES……49

TABLE. 3.10. AMOUNT OF STABILIZER NEEDED TO STABILIZE Bi_2O_3 NANOPARTICLES……51

TABLE. 3.7. STOCK SOLUTION FOR DLS ANALYSIS OF Bi_2O_3 NANOPARTICLES……51

TABLE. 3.8. AVERAGE DIAMETER OF Bi_2O_3 NANOPARTICLES WITH DIFFERENT STABILIZERS……52

LIST OF FIGURES

Figure 2.1 Main components of SEM and the kind of image acquired…… 16

Figure 2.2 Main components of TEM and the kind of image acquired…… 17

Figure 2.3 Determination of crystalline structure by XRD…….. 19

Figure 2.4 DLS system used to measure particle size and associated instrumentation….20

Figure 2.5 Mechanism of stabilization…… 33

Figure 2.6 HLB Scale showing classification of surfactant function……34

Figure 3.1 Solubility of different stabilizers in toluene…… 36

Figure 3.2 MgO nanoparticles with different stabilizers after 3 days of settling……. 38

Figure 3.3 DLS images of MgO nanoparticles…….……. 42

Figure 3.4 CeO_2 nanoparticles with different stabilizers after 3 days of settling……. 44

Figure 3.5 TEM image of CeO_2 with PIBSA……..……. 45

Figure 3.6 DLS images of CeO_2 nanoparticles…….…….47-48

Figure 3.7 Bi_2O_3 nanoparticles with different stabilizers after 3 days of settling……. 50

Figure 3.8 DLS images of Bi_2O_3 nanoparticles…….…….52-53

NOMENCLATURE

MONs	Metal oxide Nanoparticles
NP	Nanoparticles
TEM	Transmission electron microscope
XRD	X-Ray Diffraction
DLS	Dynamic light scattering
PEG	Polyethylene glycol
PVP	Polyvinyl pyrrolidone
PVA	Polyvinyl alcohol
RPM	Revolutions per minute
TOFA	Tall oil fatty acid
PIBSA	Polyisobutylene succinic anhydride
LABSA	Linear alkyl benzene sulfonic acid
Alphox	Nonyl phenol ethoxylate

CHAPTER 1

INTRODUCTION

1.1 BASICS OF NANOTECHNOLOGY

Nanotechnology is synthesis, manipulation and modification of material in the dimensions between 1 to 100 nanometers, to create nanomaterial which can be used for novel applications. As per another definition, nanotechnology refers to controlling the arrangement of individual atom or a group of few atoms. Nanotechnology is a rapidly growing field with many governments and industries worldwide spending billions of dollars on the research and development. Material at nanoscale exhibits very different properties than its bulk state and hence can have novel applications for the betterment of humanity.

Renowned physicist Richard Feynman is called the father of nanotechnology. He, in his famous 1959 Caltech talk, "There Is Plenty of Room at the Bottom"[1], predicted that one day it would be possible to assemble structures atom by atom or write the whole of Encyclopedia Britannica on the head of a pin. It was Norio Taniguchi from the University of Tokyo who stated the original definition of nanotechnology in 1974. Nanotechnology can be broadly defined science and technology of making and understanding nanomaterials, nanotools, nanomachines and nanosystems in order to solve complex problems. Even after vast development in the field of nanotechnology in recent past there are still a lot of unanswered questions related to strange properties of nanomaterials. Nanoscientists and nanotechnologists are trying to find answers to these question and exploring the wide potential of nanoscience and technology in the wide spectrum of areas such as in medicine for drug delivery, in electronics for making water proof mobile phones by silica nanocoating, in energy production by making quantum dot coated solar cells etc.

1.2 APPLICATIONS OF NANOTECHNOLOGY IN THE FIELD OF REFINING AND PROCESSING

Refining and petrochemical industry has also benefited by development of nanotechnology. Various catalyst in the form of nanomaterial have been used in the refinery industry for upgradation of hydrocarbons. Some of the important applications of nanotechnology in refining and petrochemical industry are [3, 4]:

- Development of mesoporous catalyst materials like MCM-41 for refinery purposes.
- Removal of harmful toxic substances such as nitrogen oxides, sulfur oxides, and related acids and acid anhydrides from vapor, and mercury from soil and water by use of metal oxide nanoparticles.
- Carbon capture and long-term storage using Metal organic frameworks (MOF).
- Development of a new generation of nano-membranes to enhance separation of gas streams and to remove impurities from oil.
- Upgrading of bitumen by use of clay nanoparticles.

CHAPTER 2
LITERATURE REVIEW

2.1. NANOPARTICLES AND NANO SCALE MATERIALS

The study of materials at nanoscale (1–100 nm) has gained importance after the realization that properties of materials have a strong dependence on their inherent shape and size[5]. Nanotechnology enables us to vary the size, shape, surface, composition etc. of material during synthesis to create nanomaterials with new properties having potential for several applications. Nanomaterials can be produced either from pure elements or form their compounds. Bulk materials showing properties confined to specific groups e.g., metals, semiconductors and insulators behave differently when they are transformed into nanomaterials and the new properties are dependent upon their shape and size making them suitable for entirely new applications. Some of the examples of nanomaterials are:

Nano scale metals - Nano-gold, Nano-silver, Nano-copper, Nano-iron [6,7]

Nano metal oxides - Aluminum oxide, Titanium oxide, Zinc oxide, Iron oxide [8, 9]

Semiconductors - Quantum dots [10, 11]

Nano Carbon - Carbon nanotubes, Graphene [12, 13]

2.2 SYNTHESIS TECHNIQUES FOR NANO PARTICLES

Production of nanoparticles requires careful selection of experimental technique and parameters to have

(i) uniform size and shape of the nanoparticles

(ii) uniform surface morphology

(iii) uniform crystal structure and chemical bonding properties

If these conditions are met then the synthetic process is considered as reproducible and is a reliable technique.

Today, there are many techniques available for manufacturing of nanoparticles and nanoscale structures from solids, liquids, and gases. The **Solid phase base techniques** used to manufacture of nanoparticles are straightforward and usually use Attrition techniques e.g., grinding, milling and ablations. **Liquid phase based techniques** include Hydrothermal synthesis, Co-precipitation, Sol-gel processing, Micro-emulsion, Reverse micelle synthesis, Microwave synthesis, Ultrasound synthesis, and Template based methods. **Gas-phase based techniques** are generally carried out by vaporizing a precursor material in a suitable atmosphere followed by rapid cooling, which produces super-saturation and condensation to produce nanoparticles and nanomaterials.

The techniques to produce nanomaterials can also be classified as **(i) Top-down method and (ii) Bottom-up method.** Milling, molecular beam epitaxy and photolithography are some of the well-known techniques of top down approach. Top down approach some time associated with their own disadvantages such as difficulty in producing uniform size, shape and morphology. These techniques are capital intensive and require highly specialised equipment.

Bottom-up approaches are more widely used because of easy of synthesis and uniformity in size, shape and morphology of nanoparticles. Some of the most common methods used in bottom-up approach are: **1) Co-precipitation 2) Colloidal Method 3) Sol gel method 4) Micro emulsion 5) Chemical Vapour deposition 6) Template based synthesis 7) Ultrasonic synthesis 8) Microwave synthesis.**

2.2.1 CO-PRECIPITATION METHOD: Co-precipitation is a phenomenon where a solute (e.g., water soluble metal salt), that would normally remain dissolved in a solution, precipitates out on a carrier (e.g., a base or acid) that forces metal ions to bind with each other rather than remaining dissolved [14]. In the present study the synthesis of the metal oxide nanoparticles will be done

mainly by the co-precipitation method.

2.2.2. COLLOIDAL METHOD: Metallic NPs can be produced by using the aqueous reduction of soluble metallic complexes to create colloidal suspensions of NPs. The synthesized NPs have very high surface energies and will tend to agglomerate and form larger structures to reduce their surface energy [15]. To prevent their agglomeration a stabilizer in the form of a surfactant or an organic polymer is added. Correct combination of metal complex and surfactant or capping agent enables the formation of metallic NPs.

2.2.3. SOL-GEL METHOD: Sol-gel method is similar to the two methods described above. The difference lies in the formation of interlaced network of linked particles after precipitation of agglomeration. The degree of interconnection of precipitated particles in the solvent network determines whether system will be solid or semisolid[16]. Four stage sol-gel method can be used to synthesize crystalline ZnO NPs, with zinc acetate di hydrate [$Zn(CH_3COO)_2.2H_2O$] as the source of zinc ions. The four stages consist of (i) solvation, (ii) hydrolysis, (iii) polymerization and (iv) transformation to produce ZnO NPs. In the first and second stages, ethanol is used as a solvent to dissolve the zinc acetate di hydrate in presence of monoethanolamine (MEA) which acts as a base as well as a complexing agent. In the third stage, acetate ions are removed to produce a colloidal-gel-like material and the ethanol molecules react to produce a polymer precursor with the zinc, which ultimately produces the ZnO NPs in the final stage. The final stage can be a heating process to form other ZnO nanostructures.

2.2.4 MICRO EMULSION TECHNIQUE: Oil and water are immiscible with each other and separate out into two phases when mixed. Each layer gets saturated with traces of the other component. Energy is required to combine 2 immiscible phases. High interfacial tension (30-50 dynes/cm) between bulk oil and water prevents their mixing. This interfacial tension can be

reduced by use of an amphiphilic molecule called surfactant. The hydrophilic group of surfactant interacts with water and the lipophilic group interacts with oil and get adsorb at the water-oil interface forming an emulsion. Emulsions are generally turbid when the droplet sizes ranges from 0.1 to 1 micron. Base on type of surfactant the continuous and dispersed phases are formed in emulsion. Micro-emulsion method is one of the recent techniques for the preparation of inorganic nano-particles [17] where the nanomaterials are enclosed inside the dispersed phase.

2.3. CHARACTERIZATION TECHNIQUES OF NANOPARTICLES

Development of new characterization tools that enabled us to see at molecular or atomic level has immensely contributed in development of nanotechnology. Some of the most important tools to characterize nanomaterials are (i) Scanning electron microscopy (SEM), (ii) Transmission electron microscopy (TEM), (iii) Scanning tunneling microscope (STM), (iv) Atomic force microscope (AFM), and Dynamic Light Scattering (DLS). Other conventional tools like X- Ray Diffraction (XRD), UV-Vis Spectroscopy, Thin layer chromatography (TLC), Raman Spectroscopy are also used in characterization of nanomaterials. In the present study we will be using DLS and TEM for characterization of metal oxide nanoparticles.

2.3.1 SCANNING ELECTRON MICROSCOPY (SEM)

The SEM is an instrument that uses electrons instead of photons of light to form high-resolution images (micrographs) [18]. Its components are similar to the optical microscope, but instead of glass lenses, electromagnetic lenses are used to focus the electron beam onto the sample's surface [19]. The electron beam interacts strongly with the electrons of the surface atoms in the sample. When the electron beam is focused onto the sample, the resulting illuminated pear-shaped region, known as the interaction volume, penetrates into the surface as seen in Fig 2.1.

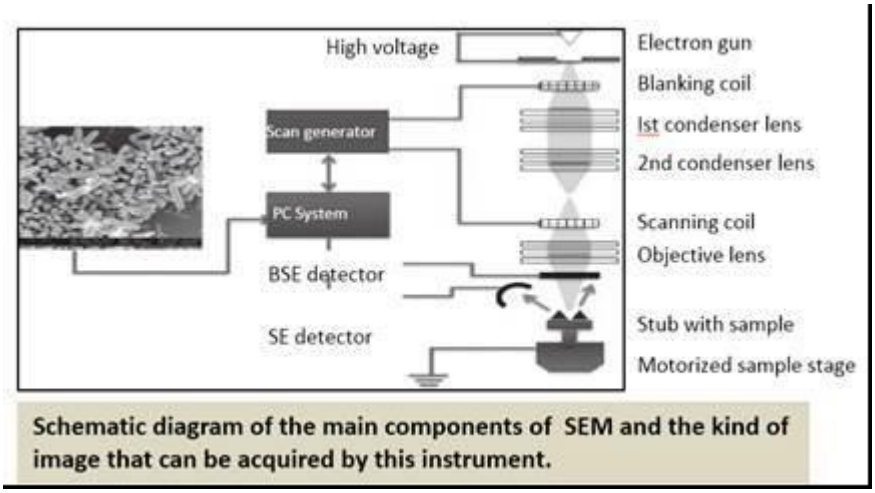

Fig 2.1 Main components of SEM and the kind of image acquired [18]

During the beam-surface interaction, several mechanisms take place, such as those involving secondary electrons (SEs), backscattered electrons (BSEs) and X-rays. BSEs are used to create compositional maps of the specimen. In addition to the SEs and BSEs, the SEM also produces characteristic X-rays, which can be used to determine the elements present in the sample material.[18]

2.3.2 TRANSMISSION ELECTRON MICROSCOPE

In 1931, Knoll and Ruska developed the TEM. The operating principle of the TEM is similar to SEM except that the detector is a phosphor screen or plate capable of capturing the image. In the case of the TEM, energetic electrons from the source are accelerated as they pass through a set of condenser lenses toward the sample. The electrons then pass through the sample, which means that the sample being analyzed must be thin enough for electron transmission to take place. During their passage, the electrons are scattered and must be collected and then focused by a set of objective lenses. The electrons are then magnified by a set of magnifying lenses (projector lens) before being projected onto a phosphor screen as presented in Figure 2.2.

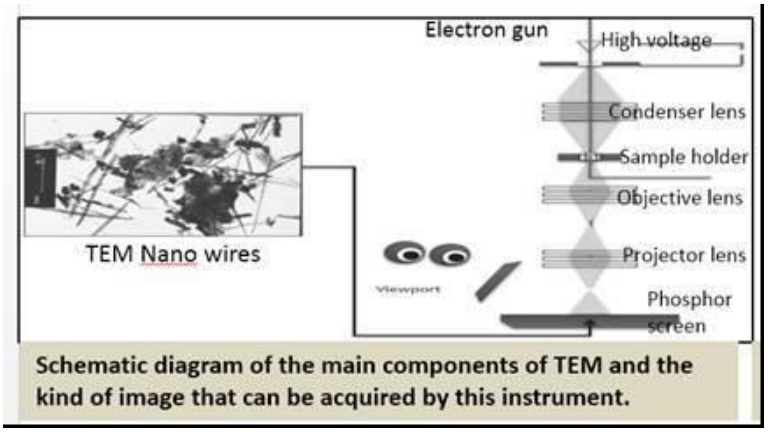

Fig 2.2 Main components of the TEM and the image acquired [18]

TEM can resolve features around 0.2 nm, which is close to the atomic radius of some materials. The low atomic weight materials appear light on the screen, while the high atomic weight materials will appear darker. [18]

2.3.3. X- RAY DIFFRACTION

X-ray diffraction is a nondestructive method used in material, physical, chemical and biological sciences to identify and quantitatively determine the crystalline phases present in a solid sample. Powder XRD is a technique specifically developed to characterize the crystallographic structure, crystallite size and preferred crystal orientations in powdered solid samples. The atomic centers in the crystal lattice act as point diffractors when the X-ray beam illuminates the sample material. Each of the diffracted X-ray beams corresponds to a coherent reflection, called a Bragg reflection, created by the atomic planes containing the atoms with the crystal. When an X-ray source of known wavelength λ is sent through an unknown crystal structure, the diffracted beam angle is predicted by the Bragg equation. [18] $n\lambda = 2d \sin \theta$ Where n is any integer, λ is the wavelength of the incident X-rays, d is the interplanar spacing, and θ is the diffraction angle. [18]

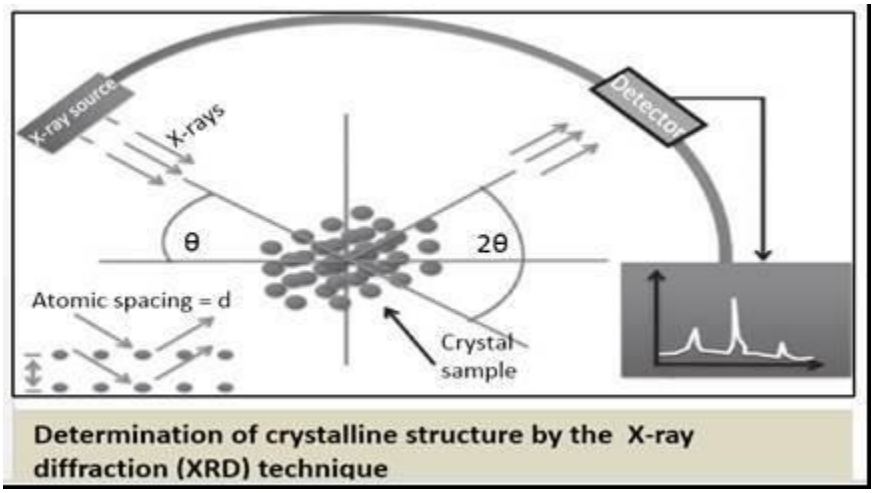

Figure 2.3: Determination of crystalline structure by XRD [18]

2.3.4. DYNAMIC LIGHT SCATTERING

Particles suspended in solution or dispersed in a solvent are always in constant motion because of Brownian motion. Random collisions between solvent molecules and particles will also affect this motion. Therefore, small particles will move faster compared to larger (heavier) particles. If the particles are very small compared to the wavelength of light, then the intensity of the scattered light will be uniform in all directions (Rayleigh scattering). However, when the particles are larger than 250nm in diameter, the intensity of the scattered light is dependent on the scatter angle (Mie scattering). If a monochromatic light in the form of a laser is used, then it is possible to record time-dependent fluctuations in the scattered intensity using a photomultiplier detector.[18] Figure 2.4 presents a schematic diagram of the typical DLS system used to measure particle size.

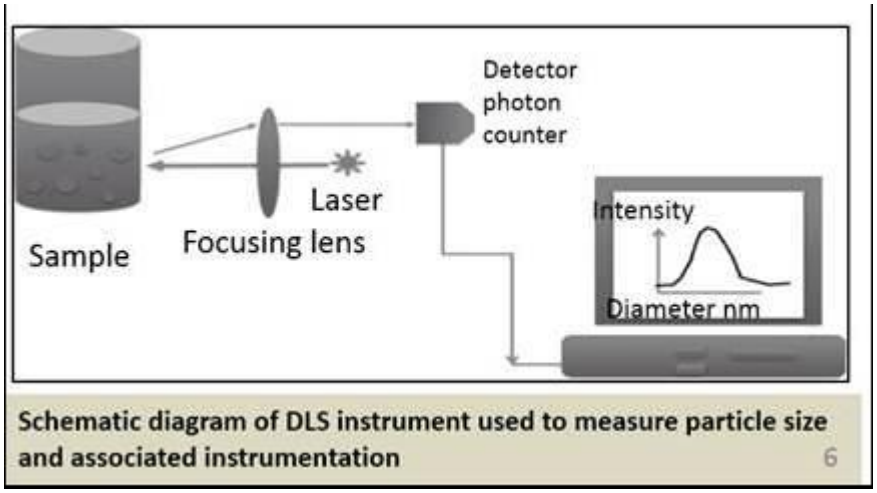

Fig 2.4 DLS system used to measure particle size and associated instrumentation [18]

2.4. LITERATURE REVIEW ON SYNTHESIS AND CHARACTERISATION OF METAL OXIDE NANOPARTICLES

2.4.1 BACKGROUND

The production of **Metal Oxide Nanoparticles (MONs)** has gained importance due to their utilization in several areas such as cosmetic, medicals and other high end applications. Zinc oxide MONs are extensively used in sunscreen, Iron oxide MONs are used as contrast agent in MRI & adsorption and decomposition of pollutants from waste water, titanium oxide MONs are used in self-cleaning mirrors. MONs are used as catalysts in several refining processes e.g., Cerium oxide MONs are being used as catalyst for complete combustion of hydrocarbons and zirconium oxide nanoparticles for inert coating in furnaces.

2.4.2. LITERATURE ON SYNTHESIS OF IRON OXIDE NANOPARTICLES

METHOD 1: Mixture of FeCl3 and FeCl2 were broken down in deoxygenated refined water and mixed for a hour. At that point 2M NaOH arrangement was included under N2 at 30˚C and the response blend was kept at 70˚C for 5 hours at 12 pH. Washing with refined water to keep up pH 7. At long last stove dried at 61-71˚C The XRD investigation demonstrated molecule estimate in the scope of 5-20 nm. The nanoparticles demonstrated immersion attractive of 89.46 emu g-1, which showed super paramagnetic properties.[23]

METHOD 2: Anhydrous FeCl3 and potassium iodide were independently broken down in water. Both arrangements were blended at room temperature, mixed and permitted to achieve harmony for 60 minutes. The hasten of iodine is sifted through, washed with refined water, dried at 100˚C. The washing was added to the filtrate. The entire volume of filtrate was then hydrolyzed utilizing 25% watery NH3 which was included drop savvy with nonstop blending until finish precipitation (pH = 9-11). The shade of the got hasten was dark attractive. The setup was left to settle, washed with refined water, dried at 250˚C. The XRD investigation indicates cubic formed molecule measure in scope of 7.84± 0.5 nm.[24]

METHOD 3: FeCl2.4H20 was included into a cup with refined water at 90˚C under blending. To this arrangement weaken ammonium hydroxide arrangement was included gradually. The accelerate got was cooled, the supernatant fluid is emptied. After centrifugation of the hasten at 5000 rpm the supernatant fluid was permitted to go through channel paper taken after by exchange of precipitation. The encourage was washed with ethanol and permitted to uncover in air for 24 hours where, it transforms into dark magnetite stage. The hasten was dried at 100˚C for 1 hour in vacuum. The XRD design showed that the particles are in crystalline frame having molecule size of 5.6 to 8.16nm.[25]

2.4.3 LITERATURE ON SYNTHESIS OF ZINC OXIDE NANOPARTICLES

METHOD 1: To the fluid arrangement of zinc sulfate, sodium hydroxide arrangement was included drop astute in a molar proportion of 1:2 under overwhelming blending for 12 h. The encourage got was separated and washed altogether with deionized water. The encourage was dried in a broiler at 100°C and ground to fine powder utilizing agate mortar. The powder gotten from the above strategy was calcined at various temperatures, for example, 300°C, 500°C, 700°C, and 900°C for 2 hr. The XRD and SEM comes about demonstrate that as the temperature of the calcinations expands, the crystallinity of the accelerate increments. The crystallite estimate acquired is 64nm, 74nm, 131nm, 187nm at 300˚C, 500˚C, 700˚C and 900˚C, individually. [26]

METHOD 2: The zinc nitrate 0.4M and NaOH (0.9M) solution were mixed and exposed to microwave irradiation for the preparation of ZnO nanoparticles. The synthesized ZnO nanoparticles were characterized by the XRD, SEM, UV-Vis and FTIR spectroscopy.[27]

METHOD 3: 0.002 moles NaOH and 0.003 moles Triethylamine were added in 950 ml of absolute ethanol, the mixture was stirred, until homogenous solution was obtained. 0.001 moles

of zinc acetate was added to alkaline solution, under magnetic stirring at 60-70˚C and this solution was continuously heated for 1 to 2 hours. It was then allowed to cool naturally at room temperature. After the reaction was complete, the resulting white product was washed with ethanol, filtered and dried in an oven at 60˚C for 3 hours. The material was then heated in a furnace at 500˚C and 800˚C for 1 hour. XRD showed the size of the synthesized nanoparticles was in the range of 14-20 nm. The SEM characterization showed that the size of the particles obtained was uniform and the shape was spherical. The crystallinity increased with temperature. [28]

2.4.4. LITERATURE ON SYNTHESIS OF COPPER OXIDE NANOPARTICLES

METHOD 1: Copper nitrate was dissolved in deionized water to form 0.1M solution. 0.1M NaOH was added drop wise to the above solution under vigorous stirring until the pH becomes 14. Black precipitate obtained were filtered and washed several times with deionized water and absolute ethanol until the pH becomes 7. The washed precipitate was dried at atmospheric pressure and 80˚C temperature for 16 hours. The precipitate was calcined at 500˚C for 4 hours. XRD showed good crystallinity of copper oxide.[29]

METHOD 2: Cupric chloride in ethanol was mixed with ethanolic solution of NaOH at room temperature. The black precipitate obtained was filtered by centrifugation, washed with ethanol and deionized water to remove NaCl salt. The precipitate was dried at 50˚C and annealed at 200˚C-600˚C. In XRD, the particle size of copper oxide at 200˚C, 400˚C and 600˚C was 15.22nm, 16.44nm and 32.50nm, respectively. XRD peak was highest at 600˚C and lowest at 200˚C suggesting that crystallinity of copper oxide nano particles increased with increase in annealing temperature.[30]

METHOD 3: Copper metal chips were dissolved in Nitric acid and the color changed from green to greenish brown. The solution was diluted with distilled water until the color changes to blue. 10% NaOH solution was added drop wise until 10pH. The precipitate was filtered and washed with distilled water several times, air dried and calcined at 150-600˚C for 3 hours to get black colored powder. In XRD analysis, the particle size obtained was 16-30nm. Crystallinity increases with increasing temperature. [31]

2.4.5. LITERATURE ON SYNTHESIS OF BISMUTH OXIDE (Bi_2O_3) NANOPARTICLES

METHOD 1: Bismuth Nitrate was dissolved in Nitric Acid. The solution was mixed with Urea in 1:5 molar ratio. The solution was heated in a water bath at 373 K. White precipitate was formed after evaporation of water. The precipitate was decomposed at temperature 400-700˚C. The powder started to swell and fill the beaker producing a foamy precursor having Bismuth oxide (Bi_2O_3) nanoparticles. The XRD sample showed crystalline pattern. The calculated lattice parameter by least square fit were a= 7.732, c = 5.618. The surface area of powder was 100 m^2/g and the average particle size is 50nm.[32, 33]

METHOD 2: Solution A was prepared by the addition of HNO_3 to Bismuth nitrate. NH_4OH was added drop wise to precipitate Bismuth hydroxide. The hydrated Bismuth hydroxide was washed to remove all the anions and then transferred to flask which was fitted with a water condenser. The gel was continuously stirred for 6 hours at 70-100˚ C. The crystalline powder was filtered and oven dried overnight. $Bi(OH)_3$ precipitate was allowed to decompose at 200-500˚C for 12 hours to form Bi_2O_3. The XRD sample showed crystalline pattern. The calculated lattice parameter by least square fit were a= 7.736, c = 5.614. The surface area of powder is 90m^2/g and the average particle size is 50nm. [34]

2.4.6. LITERATURE ON SYNTHESIS OF ANTIMONY OXIDE NANOPARTICLES

METHOD 1 $SbCl_3$ was dissolved in 1 M HCl solution and small amount of PVA was added to it. The mixture was ultrasonically vibrated for 15 minutes, followed by addition of NaOH solution slowly until the mixture becomes transparent pale yellow. The solution was refluxed for 1 hour to get more intense color. During refluxing the solvent was evaporated at 80˚C under vacuum. TEM analysis showed the crystalline structure was cubic and the crystallite size was 10-80nm. [35]

METHOD 2: Cetyl Trimethyl Ammonium Bromide was added into 0.01 M $SbCl_3$ under constant stirring, for 2 hours until the Cetyl Trimethyl Ammonium Bromide (CTAB) was fully dissolved. To make the pH of solution up to 14, 1 M NaOH solution was added drop wise in the above mixture. The solution was stirred for 24 hours at room temperature and then at 60˚C for 4 hours. The light brown precipitate obtained was centrifuged and washed multiple times with ethanol and distilled water. The precipitate was dried under vacuum at room temperature. In the XRD analysis, the crystalline structure was cubic and the crystallite size was 17nm. [36]

2.4.7. LITERATURE ON SYNTHESIS OF MAGNESIUM OXIDE NANOPARTICLES

METHOD 1: Magnesium chloride was dissolved in de-ionized water and heated to 70˚C. Then macro crystalline magnesium oxide was added in about 30 minutes, at 5 minutes intervals, and the content was stirred for about 21 hours. A gel was obtained which was cooled at room temperature. For preparation of Magnesium oxalate about 5ml of the gel was added into 0.1M ammonium oxalate aqueous solution and the contents were centrifuged, washed with water four times, followed by ethanol and dried in an oven. The Magnesium oxalate dehydrate thus obtained was used as the precursor to Magnesium oxide. XRD analysis showed that on increasing the annealing temperature, the crystallinity of the MgO particles increased. [38]

METHOD 2: Magnesium methoxide and toluene were placed in 100ml cylindrical reactive container with diameter 40 mm under argon atmosphere. The solution was purged with high intensity ultrasound by employing immersion titanium horn. The temperature during sonication was increased to 60˚C. During sonication 0.22ml distilled water was slowly added from syringe. After 1-2min clear gel solution was obtained and ultrasound irradiation was terminated. The hydroxide gel solution obtained after sonification was transferred into 100ml stainless steel autoclave and slowly heated to 265˚C for 15 mins. The product was removed from the autoclave and dried in the oven at 120˚C. The final product was stored in an inert atmosphere. Hydrated MgO precursors were heat treated and then allowed to cool at room temperature [39].

2.4.8 LITERATURE ON SYNTHESIS OF CERIUM OXIDE NANOPARTICLES

METHOD 1 0.1M Cerium Chloride and 0.3M NaOH were prepared separately in distilled water. NaOH solution was added drop wise to Cerium Chloride solution under constant stirring using a magnetic stirrer. The reaction was allowed to proceed for 4 hours, after the complete addition of NaOH solution under stirring at room temperature. The precipitate was washed 3 times with distilled water and ethanol. The product was dried at 100˚C for 3 hours to complete the conversion of $Ce(OH)_3$ to CeO_2. The powder was heated at 500˚C for 3 hours in a muffle furnace. In XRD analysis, cerium oxide particles were crystalline in nature and showed cubic phase structure. The particle size ranged from 18-27 nm. SEM showed agglomeration of primary nanoparticles into secondary micro particles. [40]

METHOD 2: Cerium nitrate was added to solution of NaOH. PEG or PVP was used as surfactant. This solution was stirred at room temperature for 1 hour at 1000 RPM. The yellow colored precipitate of $Ce(OH)_4$ was washed with water and ethanol 5-10 times. The precipitate was dried at 50-100˚C for 24 hours and calcined at 600˚C for 2 hours. The XRD analysis showed cubic phase structure. The SEM analysis showed that the particles were porous and the pore size of the particles ranged from 10-50 nm. Agglomerated sample exhibit a flake like morphology and the grain size was found to be 42-56nm. [41]

METHOD 3: Cerium Nitrate was dissolved in H_2O or ($C_2H_5OH+H_2O$ 1/1 vol.). The solution was heated under stirring, then NH_4OH was added. Precipitate of $Ce(OH)_3$ shown by the light brown coloration was formed because of low solubility product. As the pH was maintained at 9-9.5, the coloration of the precipitate turned into purple which characterizes the oxidation of $Ce(OH)_3$ to $Ce(OH)_4$. The reaction was stopped after 1.5 hours of vigorous stirring. The obtained precipitate was centrifuged, washed with distilled water and ethanol alternatively for 3 times. In XRD analysis, the particle sizes obtained were 10.5-19.9nm. [43]

2.4.9. LITERATURE ON SYNTHESIS OF ZIRCONIUM OXIDE NANOPARTICLES

METHOD 1: Zirconyl Nitrate and KI were mixed in 10 ml CH_3OH. Isophthalic acid was dissolved in 10 ml CH_3OH. Both these solutions were mixed together and sonicated for 30 minutes in an ultrasound vessel, to obtain homogenous mixture. Yellow precipitate formed was separated by centrifugation at 4000 RPM for 15 minutes. The precipitate was washed with double distilled water and acetone. The precipitate was calcined at 700˚C for 4 hours at atmospheric pressure to form ZrO_2 nanoparticles. The XRD and SEM analysis showed the crystal structure was tetragonal. The unit cell parameter was a = b = 3.617Å, c = 5.176Å. The unit cell volume was 67.33$Å^3$ and the crystallite size in XRD was 51nm and in SEM was 49nm. [44]

METHOD 2: Zirconium Oxychloride was dissolved in distilled water (0.025 M). The solution was hydrolyzed by drop wise addition of Aq. NH_3 under continuous stirring until pH became 10-10.5. The precipitate formed was filtered and washed with distilled water, until it became free from chloride ion. Precipitate was dried at 110˚ C for 12 hours. The sample prepared was

calcined at 400˚C for 4 hours to form ZrO_2 nanoparticles. The crystal structure was tetragonal and the crystallite size was 11-13nm. [45]

METHOD 3: Zirconium Oxychloride and NaOH were used for the preparation of nano ZrO_2. Zirconium oxychloride was dissolved in distilled water using hot plate magnetic stirrer. Aqueous solution of 2M NaOH was mixed in the above mentioned precursor solution until the pH value becomes 8. The precipitate was filtered after 15 minutes and was cleaned with water and acetone many times and then it was dried at 100°C overnight. The calcination of the ZrO2 was done at 700°C, 1000°C and 1200°C. The XRD samples show that the crystallite size increased as a function of annealing temperature. The average grain size of the crystalline samples are 25nm, 42nm and 46nm respectively.[46].

METHOD 4: $ZrCl_4$ was dissolved in distilled water (0.06M). Different quantities of template (poly ethylene glycol 4000, urea and sorbitol) were added separately to the desired amount of ammonia solution and well mixed by stirring for 5 minutes. The prepared solution was added drop wise to $ZrCl_4$ solution at room temperature under stirring. The mixture was heated 60˚C or 70˚C or 80˚C and kept for few minutes. As the reaction completed, white solid products were washed with distilled water and ethanol to remove the ions possibly remaining in the final products, and finally dried at 60˚C. The product was calcined at 550˚C for 2 hours. In the TEM images, the average particle size of the samples was about 6.59nm. [47].

2.4.10. LITERATURE ON SYNTHESIS OF MOLYBDENUM OXIDE NANOPARTICLES

METHOD 1: Ammonium Heptamolybdate and urea were separately dissolved in distilled water. Then urea solution was added to Mo salt solution slowly and pH of the reaction mixture was maintained by using ammonium hydroxide solution. While stirring the solution is heated to 80^oC until the solid precipitate was formed. The precipitate was dried to 100^oC in oven for 6 hrs. The dried precipitate was heated to 250^oC in a furnace with the rate of 5^oC/min for 1 hour in the presence of air. Finally it was heated to 500^oC for 90 minutes. SEM analysis showed that as the annealing temperature increased the crystal size also increased. [48]

2.5. LITERATURE ON STABILISATION OF METAL OXIDE NANOPARTICLES

As nanoparticles are essentially finely divided materials, they are thermodynamically unstable

with respect to agglomeration. Consequently, they need to be kinetically stabilized and this is typically done using a protective stabilizer. The stabilization is achieved by electrostatic or steric forces or a combination of the two (electro steric forces). The stabilizer is typically introduced during the formation of the nanoparticles, and this is achieved via the chemical or electrochemical reduction or thermal decomposition of metallic precursors. The subsequent interaction between the stabilizer and the surface of the nanoparticle is a highly dynamic one, with its strength and nature often controlling the long-term stability of a dispersion of the nanoparticles.

2.5.1 AQUEOUS TO HYDROCARBON PHASE TRANSFER

In our study, MONs will be synthesized by simple co-precipitation method in aqueous medium and their end use may be in hydrocarbon medium. Therefore, we need to transfer the nanoparticles from either directly from aqueous medium or after calcination in solid form to organic/hydrocarbon phase.

Different stabilizers are required to make stable dispersion of nanoparticles in hydrocarbon phase. These stabilizers may be small surfactant molecules (e.g., Linear Alkyl Benzene Sulphonic Acid, LABSA) or polymeric molecule (e.g., Polyisobutylene Succinic Anhydride, PIBSA). Oleic acid has been used as stabilizer for stable dispersion of CeO_2 nanoparticles in hexane, decaline, octyl ether, 1-tetradecene.[49]

2.5.2. MECHANISM OF STABILISATION

Surfactant (small molecule or polymer) based stabilization:

As shown in Fig. 2.5, the surfactant helps to reduce the interfacial tension between the surfaces. It forms micelles, in which head is hydrophilic and tail is hydrophobic. The hydrophilic part is attached to the nanoparticle and hydrophobic part remains suspended in organic phase.

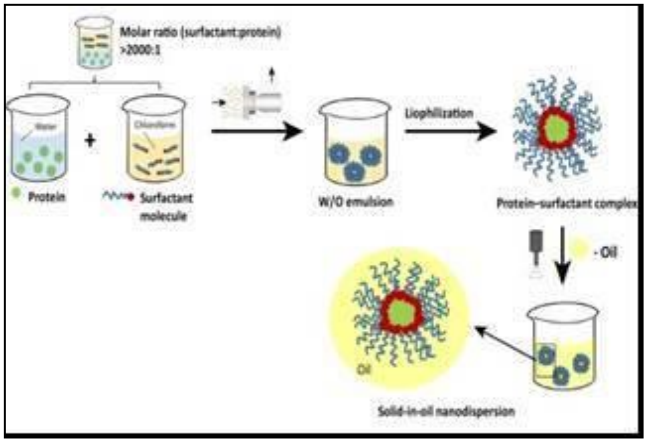

Fig 2.5 Mechanism of stabilization [www.wikipedia.com]

2.5.3 HLB VALUE OF A SURFACTANT

The hydrophilic-lipophilic balance (HLB) of a surfactant is a measure of the degree to which it is hydrophilic or lipophilic, determined by calculating values for the different regions of the molecule. It can be calculated by the following two methods:

Griffin's Method

HLB = 20*M_h/M, where M_h is the molecular mass of the hydrophilic portion of the molecule, and M is the molecular mass of the whole molecule.

Davies Method

$$HLB = 7 + \sum_{i=1}^{m} H_i - n * 0.475$$

Where m is the number of hydrophilic groups in the molecule, H_i is the value of the i^{th} hydrophilic groups and n is the number of lipophilic group in the molecule.

A classification system as shown in Fig 2.6 has been developed that gives the surfactant function.

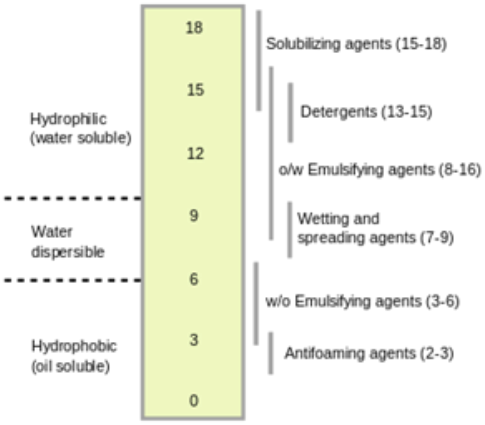

Fig. 2.6. HLB Scale showing classification of surfactant function [www.wikipedia.com]

Table 2.1 shows various stabilizers used in this study and their HLB values. Among these the HLB value is the highest for Alphox-400 and lowest for PIBSA.

TABLE 2.1. HLB VALUE OF VARIOUS STABILIZERS

Name	Mol. Wt	Mol. wt of hydrophilic group	HLB (by Griffin's Method)
LABSA	326	81	5
PIBSA	950	99	2.1
TOFA	285	45	5
Alphox 50 (n= 2)	308	89	6.8
Alphox 100 (n= 4.5)	418	199	9.1
Alphox 200 (n=9.5)	638	419	13.1
Alphox 400 (n=20)	1100	881	16
PVA	44	17	7.7

CHAPTER 3

MATERIALS AND METHODS

Cerium Nitrate of 99% purity, Magneisum chloride of 99% purity and Bismuth Nitrate of 98% purity were procured from Sigma Aldrich. All metal salts were used without any further purification. Commercial grade Polyisobutylene succinic anhydride (PIBSA), Tall oil fatty acid (TOFA), Nonyl phenol ethoxlate (Alphox) and Linear alkyl benzene sulfonic acid (LABSA) were used as stabilizers. All solvents of LR grade were used for synthesis and washing of nanoparticles.

Nanoparticles were synthesized using co-precipitation technique. The alkaline solution was taken in a dropping funnel and the metal salts were taken in round bottom flask with magnetic stirrer for contant stirring of reaction mixture. The details of experimental procedue is mentioned for each metal oxide nanoparticle in the next section.

After completion of the reaction the precipitated nanoparticles were filtered in a buchner funnel with Whatman 41 filter paper. The precipitated nanoparticle were washed 4 times with DM water and finally with methanol.

The washed nanoparticles were dried at 80-120°C in a hot air oven and calcined at 300-500°C in a muffel furnace.

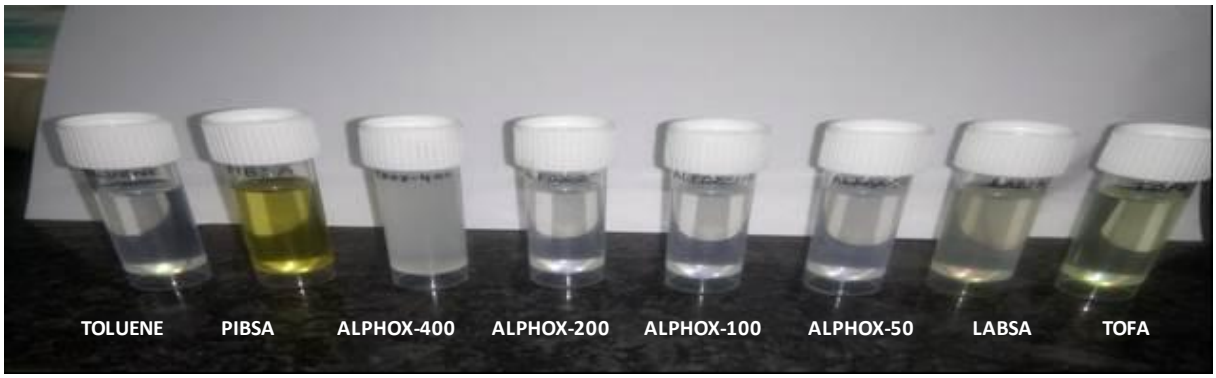

Fig 3.1: Solubility of different stabilizers in toluene

All stabilizers used in this study were dissolved in toluene to check solubility. Figure 3.1 shows all stabilizers except Alphox 400 were completely miscibile with toluene. Alphox 400 made a hazy solution with toluene

3.1. SYNTHESIS OF MgO NANOPARTICLES

900 mL of 2.5wt% of NH_3 solution was added to 500mL 0.4M $MgCl_2.6H_2O$ solution. The pH

was maintained at 9-10 during reaction.The precipitated $MgOH_2$ was left for 8 hrs for digestion. Then it was filtered and washed 5 times with DM water till the filtrate was neutral on pH paper. The precipitate $Mg(OH)_2$ nanoparticles were dried in air at 100°C for 12 hrs. Then calcination was done at 500°C for 6 hrs. The yield of dried and calcined magnesium oxide nanoparticle was 60%. Table 3.1 shows the experimental data of MgO nanoparticles.

Run	**$MgCl_2.6H_2O$(g) MW 203.31g/mol**	**NH_3 (ml) MW 17 g/mol**	**Wet Cake Weight (g)**	**Dry Weight @100°C for 12 hrs (g)**	**Calcined Weight @500°C for 6 hrs (g)**	**Yield (%)**
Run-1	39.8076	900	43.8	6.3	4.5	57
Run-2	81.2978	1800	25.8923	12.0	9.6833	60

Table 3.1: Experimental details of MgO Nanoparticles

Reaction for synthesis of MgO nanoparticles

$$MgCl_2.6H_2O\ (s) + NH_3\ (Aq) \longrightarrow Mg(OH)_2\ (s) + NH_4Cl\ (Aq)$$

$$Mg(OH)_2(s) \xrightarrow{\text{Calcination at 500°C}} MgO\ (\text{Nanoparticles})$$

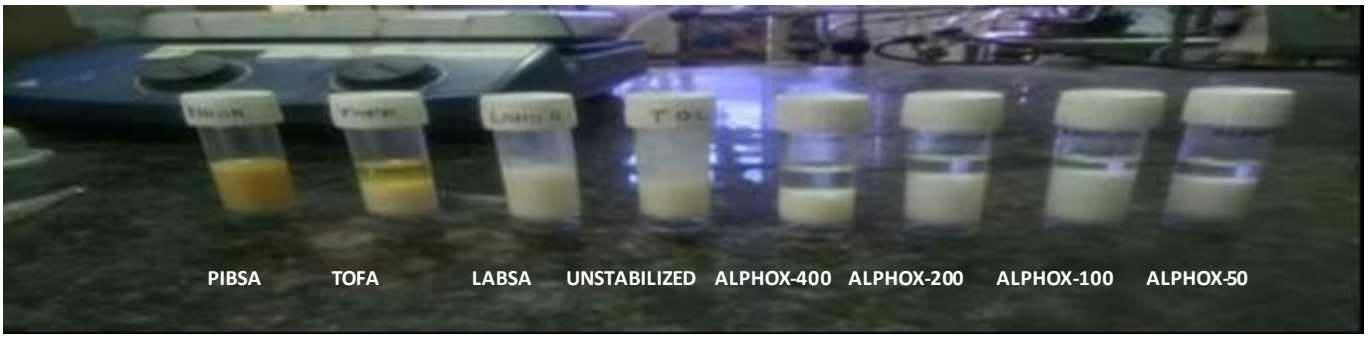

Fig 3.2 Mgo nanoparticles with different stabilizers after 3 days of settling

Stabilization of MgO nanoparticles

0.1 – 0.3g of different stabilizer were added to 5 ml toluene and 0.3g MgO nanoparticles were added to the solution and sample was sonicated for 60 minutes in ultrasonic bath. Then kept for settling for 3 days.

3.2. SYNTHESIS OF CeO_2 NANOPARTICLES

4.5794g of $Ce(NO_3)_3.6H_2O$ was dissolved in 100 ml of DM water (0.01 mole), 1.6252g of NaOH was dissolved in 100 ml DM water (0.04 mole). 1 ml (6.25 wt%) PVA solution was added to NaOH solution. Then NaOH+PVA solution was added to $Ce(NO_3)_3.6H_2O$ solution drop by drop under constant stirring by magnetic stirrer. Then the precipitate was filtered and washed 5 times with DM water and finally by methanol until the pH of the filtrate was neutral on pH paper. The precipitate CeO_2 nanoparticles were dried in air at 80°C for 24 hours. Then calcination was done at 500°C for 2 hrs. The yield of dried and calcined cerium oxide nanoparticle was 97%. Table 3.5 shows the experimental details of CeO_2 nanoparticles.

Run	$Ce(NO_3)_3.6H_2O$ (g) MW = 434.2 g/mol	NaOH (g) MW = 40 g/mol	Wet Cake Weight (g)	Dry Weight @80°C for 24 hrs (g)	Calcined Weight @500°C for 2 hrs (g)	Yield, (%)
Run-2	4.5794	1.6252	23.5678	1.3658	1.2515	68.9
Run-3	68.8023	24.3386	138.6	27.8	26.4864	97.1

Table 3.5: Experimental details of CeO_2 Nanoparticles

Reaction

$$Ce(NO_3)_3\ (Aq) + NaOH\ (Aq) \longrightarrow Ce(OH)_3\ (s) + NaNO_3\ (Aq)$$

$$Ce(OH)_3\ (s) \xrightarrow{\text{Calcination at 500°C}} CeO_2\ \text{(Nanoparticles)}$$

Table 3.6: Amount of stabilizer needed to stabilize CeO_2 Nanoparticles

Stabilizer	Amount Stabilizer (g)	Amount CeO_2 (g)	Toluene (ml)	wt% stabilizer	wt% CeO_2	Remarks
LABSA	0.3938	0.1054	10	3.938	1.054	Stabilized
PIBSA	0.4384	0.1172	10	4.384	1.172	Stabilized
TOFA	0.5511	0.1165	10	5.511	1.165	Partially Stabilized

Table 3.6 shows the amount of stabilizer needed to stabilize 0.1g of CeO_2 nanoparticles in 10 ml of Toluene

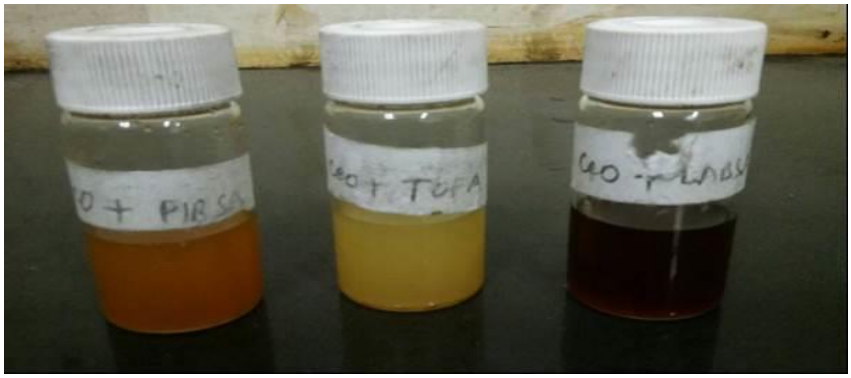

Fig 3.5: CeO_2 nanoparticles with different stabilizers after 3 days of settling

0.2 – 0.6g of stabilizer such as PIBSA, TOFA and LABSA were added to 10 ml of toluene and mixed uniformly by shaking. After that 0.1g CeO_2 nanoparticles were added to the solution and solution was sonicated for 60 minutes in ultrasonic bath and then samples kept for settling for 3 days. Fig 3.5 shows the stabilization of CeO_2 nanoparticles with different stabilizer. Following observations were recorded after 3 days of settling:

- Visually best stabilization was observed in LABSA and PIBSA.
- Order of stabilization of different stabilizers:

  LABSA > PIBSA > TOFA

3.3. SYNTHESIS OF Bi_2O_3 NANOPARTICLE

0.1M $Bi(NO_3)_3.5H_2O$ solution was prepared in 50 ml HNO_3. 25 wt% of NH_3 solution was added dropwise into $Bi(NO_3)_3.5H_2O$ solution until the pH of the solution becomes 9-10. Then the precipitate was filtered and washed 4 times with DM water and finally with methanol till the pH of the filtrate was neutral on pH paper. The precipitate $Bi(OH)_3$ nanoparticles was dried at 100^oC in air for 12 hrs. Then Calcination was done at 500^oC for 6 hrs. The yield of dried and calcined bismuth oxide nanoparticle was 47%. Table 3.9 shows the experimental details of Bi_2O_3 nanoparticles.

Table 3.9: Experimental details of Bi_2O_3 Nanoparticles

Run	$Bi(NO_3)_3.5H_2O$ (g) MW = 485.07 g/mol	NH_3 (ml) MW = 17 g/mol	Wet Cake Weight (g)	Dry Weight @100°C for 12 hrs (g)	Calcined Weight @500°C for 6 hrs (g)	% Yield
Run-1	4.0504	150	5.2108	2.1958	2.0456	52.6
Run-2	20.0680	650	22.2006	9.7832	9.1824	47.6

Reaction

$$Bi(NO_3)_3.5H_2O\ (Aq) + NH_3 \longrightarrow (Aq)\ Bi(OH)_3\ (s)$$

$$Bi(OH)_3\ (s) \xrightarrow{\text{Calcination at } 500^{\circ}C} Bi_2O_3\ \text{(Nanoparticles)}$$

Fig 3.8: Bi_2O_3 nanoparticles with different stabilizers after 3 days of settling

0.1–0.3g of different stabilizer were added to 10 ml toluene and 0.1g Bi_2O_3 nanoparticles were added to the solution and sample was sonicated for 60 minutes in ultrasonic bath and then kept for settling for 3 days. Fig 3.8 shows the stabilization of Bi_2O_3 nanoparticles with different stabilizers. Foloowing observations were recorded after 3 days of settling:

- Best stabilization was observed in LABSA and PIBSA.
- Bi_2O_3 nanoparticles were sedimenting in all other stabilizers.
- Order of stabilization of different stabilizers:

LABSA>PIBSA>TOFA>ALFOX-50>ALFOX-100>ALFOX-200>ALFOX-400

Table 3.10 shows the amount of stabilizer needed to stabilize 0.1g of Bi_2O_3 nanoparticles in 10 ml of toluene.

Stabilizer	Amount Stabilizer (g)	Amount Bi_2O_3 (g)	Toluene (ml)	wt% stabilizer	wt% Bi_2O_3	Remark
LABSA	0.3938	0.1095	10	3.938	1.095	Stabilized
PIBSA	0.4384	0.0950	10	4.384	0.950	Stabilized
TOFA	0.5511	0.1035	10	5.511	1.035	Partially Stabilized
ALFOX	0.2500	0.0543	10	2.500	0.543	Not Stabilized

-50						
ALFOX -100	0.2447	0.0947	10	2.447	0.947	Not Stabilized
ALFOX -200	0.2679	0.0919	10	2.679	0.919	Not Stabilized
ALFOX -400	0.2013	0.0993	10	2.013	0.993	Not Stabilized

Table 3.10: Amount of stabilizer needed to stabilize Bi_2O_3 Nanoparticles

4.0 Result and Discussion

Result and Discussion for MgO Nanoparticles

We have obtained 57-60% yield of MgO nanoparticles by co-precipitation method. Fig 3.2 shows the stabilization of MgO nanoparticles with different stabilizers.

Following observations were recorded after 3 days of settling:

- MgO nanoparticle formed gel in pure toluene.
- Visually best stabilization (no settling) was observed in PIBSA, TOFA and LABSA.
- MgO nanoparticles were sedimenting in all other stabilizers.
- Order of stabilization of different stabilizers:

PIBSA> TOFA>LABSA> ALFOX-50> ALFOX-100>ALFOX-200=ALFOX-400

Table 3.2 shows the amount of stabilizer needed to stabilize 0.3g of MgO nanoparticles in 5 ml of toluene.

Table 3.2: Amount of stabilizer needed to stabilize MgO Nanoparticles

Stabilizer name	Amount Stabilizer(g)	Amount MgO (g)	Toluene (ml)	wt% stabilizer	wt% MgO	Remarks
PIBSA	0.2	0.3	5	4	6	Best Stabilized
LABSA	0.1	0.3	5	2	6	2nd Best Stabilized
TOFA	0.3	0.3	5	6	6	3rd Best Stabilized
ALFOX-50	0.3	0.3	5	6	6	4th Best Stabilized
ALFOX-100	0.3	0.3	5	6	6	5th Best Stabilized
ALFOX-200	0.3	0.3	5	6	6	Not Stabilized
ALFOX-400	0.3	0.3	5	6	6	Not Stabilized

In this study, two types of stabilizers were used to disperse metal oxide nanoparticles in organic solvent.

1) Stabilizer with polar acidic functional group such as LABSA (sulfonic acid), PIBSA &

TOFA (carboxylic acid) and nonpolar hydrocarbon chains. LABSA & TOFA have linear hydrocarbon chains whereas PIBSA has branched hydrocarbon chain.

2) Stabilizers with hydrophilic ethylene oxide group and C_9 alkyl non-polar chains e.g., Nonyl phenol ethoxlate (Alphox)

MgO is basic in nature and the acidic head group of stabilizers can interact with it. The non-polar tail of stabilizers keep it soluble in the hydrocarbon solvent. Structure of both polar and non-polar group have strong effect on stabilization properties of stabilizers. For example the sulfonic acid group of LABSA can make strong bond with MgO where as carboxylic acid group of TOFA will make weaker bond. Anhydride group of PIBSA can make bidentate interation with MgO due to presence of two carboxylic acid groups.

The ethoxy head group of nonylphenol ethoxlate will interact with MgO nanoparticles due to polar-polar interaction which is weaker than the acid base interation of stabilizers having acidic functionality. As the length of ethoxy group is increased from Alphox 50 to Alphox 400 the stabilization power of stabilizer has redued drastically. Alphox 400 with 19 repeating units of ethoxy group is not miscible in toluene.

The branched nonpolar chain has better stabilization power in slightly polar aromatic solvents whereas more non-polar linear chains will have better stabilization power in nonpolar hydrocarbon solvents e.g., hexane or heptane. The chain length also plays important role as the C_{18} chain in TOFA has better stabilization than C_{12} chain in LABSA.

TEM image of MgO nanoparticle with PIBSA

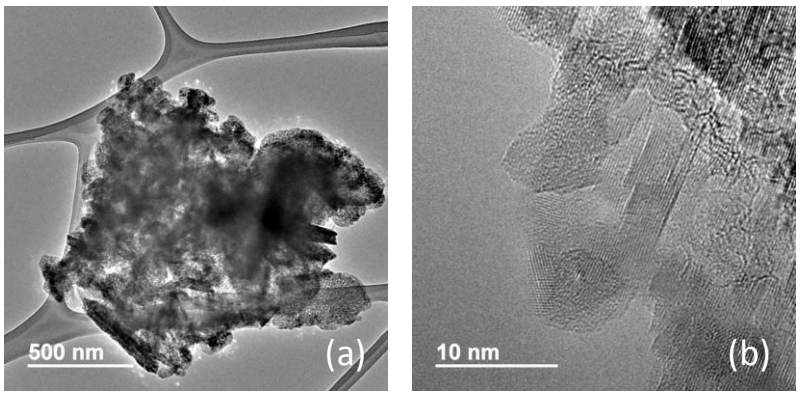

Fig 3.3: TEM image of MgO with PIBSA at (a) 500 nm scale (b) 10nm scale

Fig 3.3 shows the TEM images of MgO stabilized with PIBSA at different resolutions. Fig 3.3

(a) shows that the MgO nanoparticles are sugnificantly agglomerated and the size is >500nm. Fig 3.3 (b) shows the average crystallite size of MgO is in the range of 10-20nm.

Dynamic Light Scattering (DLS): Stock solution of MgO nanoparticles was prepared as shown in Tbale 3.3. The solution were diluted 5 times to make final nanoparticle concentration of 2mg/mL for DLS analysis.

Table 3.3: Stock solution for DLS analysis of MgO nanoparticles

Stabilizer	MgO, mg/mL	Stabilizer, mg/mL	MON to Stabilizer ratio
TOFA	10	100	1:10
PIBSA	10	100	1:10
LABSA	10	100	1:10

DLS results of MgO nanoparticles are tabulated in Table 3.4. In the case of MgO nanoparticles stabilized with LABSA, two different distributions of sizes were observed. The first peak havig 75.7% intensity has average hydrodynamic diameter of 525.9 nm and the second peak having 24.3% intensity has the average diameter of 4613 nm.
Therefore LABSA was not able to efficiently stabilize the MgO nanoparticles. Both peak 1 and peak 2 have very large average hydrodynamic diameters. In case of TOFA the average hydrodynamic diameter of majority of nanoparticles (99.4%) was much smaller i.e., 245 nm but very few nanoparticles were present as large agglomerates having average diameter of 5088 nm. In the case of PIBSA all nanoparticles have shown a single peak of average hydrodynamic diameter of 323.4 nm. Therefore the DLS data suggests that TOFA and PIBSA have better stabilization than LABSA.

Table 3.4: Average diameter of MgO nanoparticles with different stabilizers

Stabilizer	Peak 1		Peak 2		Remarks
	Avg Dia, nm	% Intensity	Avg Dia, nm	% Intensity	
LABSA	525.9	75.7	4613	24.3	Significant agglomeraton
TOFA	245	99.4	5088	0.6	Some agglomeration
PIBSA	323.4	100	0	0	No agglomeration

Figure 3.4 shows the size distribution of MgO stabilized with (a)PIBSA (b)TOFA & (c)LABSA.

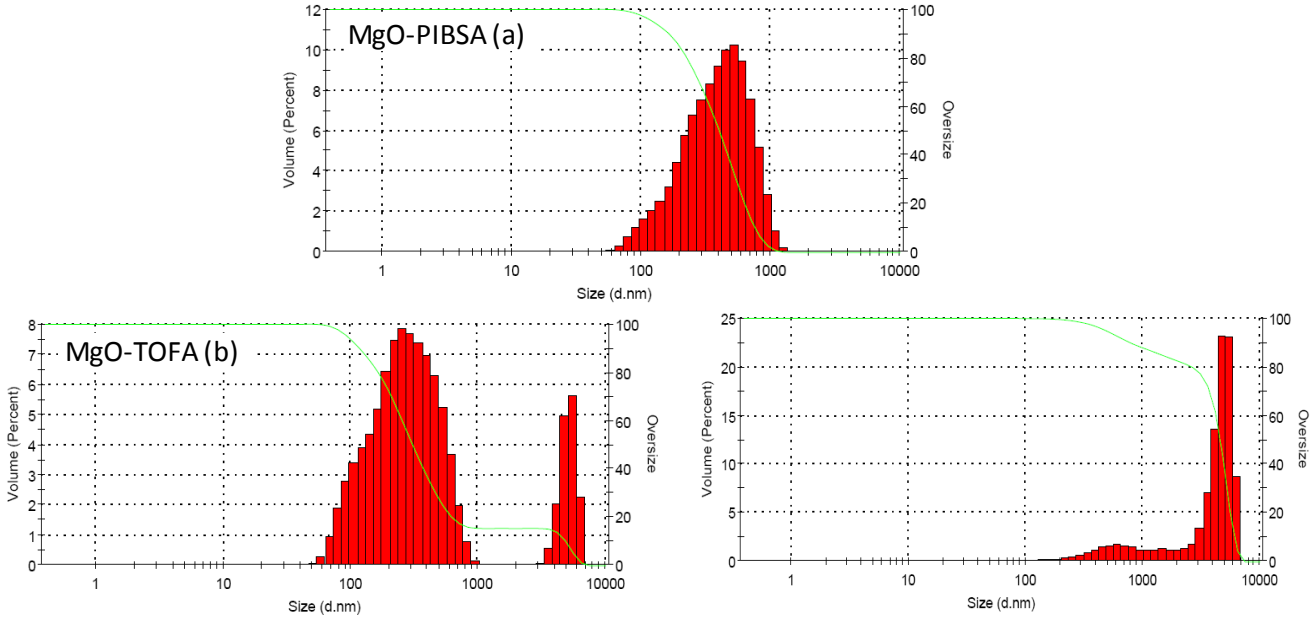

Fig 3.4: DLS images of MgO nanoparticles with (a) PIBSA (b) TOFA (c) LABSA

Result and Discussion for CeO2 nanoparticle

TEM image of CeO_2 nanoparticle with PIBSA

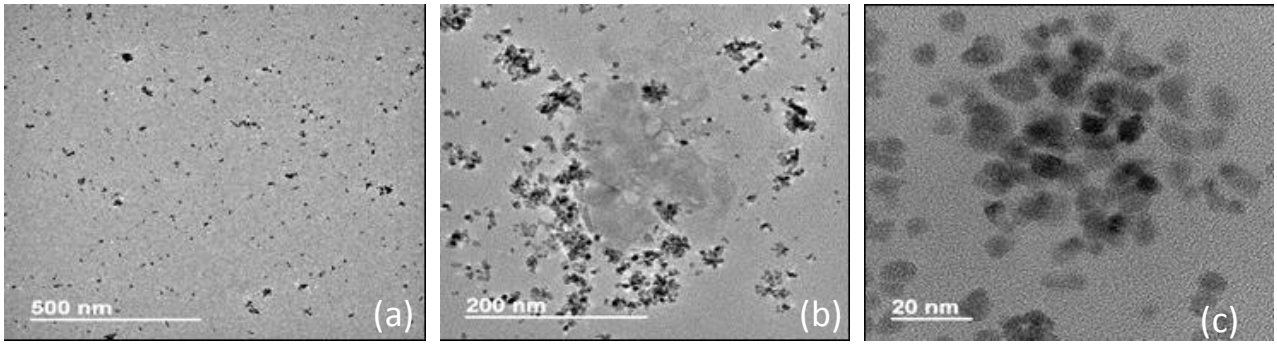

Fig 3.6: TEM image of CeO_2 with PIBSA at (a) 500nm scale (b) 200nm scale (c) 20nm scale

Fig 3.6 showing the Transmission electron microscope (TEM) image of CeO_2 stabilized with PIBSA in Toluene at different resolutions. Fig 3.6(a) shows that the CeO_2 nanoparticles are uniformly distributed and no big agglomerates (>60nm) are visible. Fig 3.6(b) shows the average particle size of agglomerated CeO_2 is 40-50 nm. Fig 3.6(c) shows that the crystallite size of CeO_2 is in the range of 5-10 nm.

Dynamic Light Scattering (DLS): Stock solution of CeO_2 nanoparticles was prepared as shown in Tbale 3.7. The solution were diluted 5 times to make final nanoparticle concentration of 2mg/mL for DLS analysis.

Table 3.7: Stock solution for DLS analysis of CeO_2 nanoparticles

Stabilizer	CeO_2, mg/mL	Stabilizer, mg/mL	MON to Stabilizer ratio
TOFA	10	100	1:10
PIBSA	10	100	1:10
LABSA	10	100	1:10

In the case of CeO_2 nanoparticles stabilized with LABSA the average hydrodynamic diameter of 82.3% particle is 167.6 nm and the average hydrodynamic diameter of 17.7% is 44.1 nm. Which suggests that most of the particles are well stabilized and no significant agglomeration has taken place. Similarly in case of CeO_2 stabilized by PIBSA majority of nanoparticles are having average diameter of 225 nm which is larger than LABSA stabilized nanoparticles.

Table 3.8: Average diameter of CeO_2 nanoparticles with different stabilizers

Stabilizer	Peak 1		Peak 2		Peak 3		Remarks
	Avg Dia, nm	% Intensity	Avg Dia, nm	% Intensity	Avg Dia, nm	% Intensity	
LABSA	167.6	82.3	44.1	17.7	0	0	No agglomeration
PIBSA	225.8	87.1	39.94	12.9	0	0	No agglomeration
TOFA	168.9	62.2	493	27.2	31.64	10.5	Some agglomeration

In case of CeO_2 nanoparticles stabilized with TOFA the average hydrodynamic diameter of 62.2% particle is 168.9 nm but 31.64% of the CeO_2 nanoparticles are showing bigger diameter of 493 nm suggesting some agglomeration. LABSA has shown better stabilized of CeO2 nanoparticles compared to other two stabilizers. The DLS spectra of CeO2 nanopartciles stabilized with different stabilizers is shown in Figure 3.7.

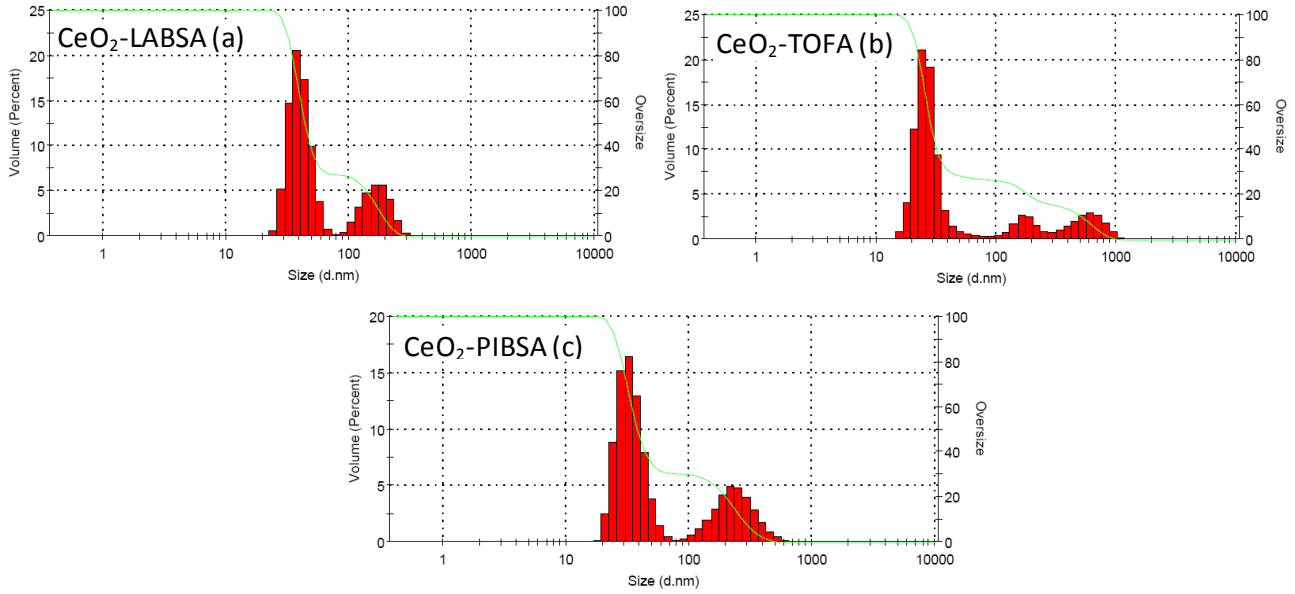

Fig 3.7: DLS images of CeO_2 nanoparticles with (a) LABSA (b) TOFA (c) PIBSA

Result and Discussion for Bi2O3 nanoparticle

TEM image of Bi_2O_3 nanoparticle with PIBSA

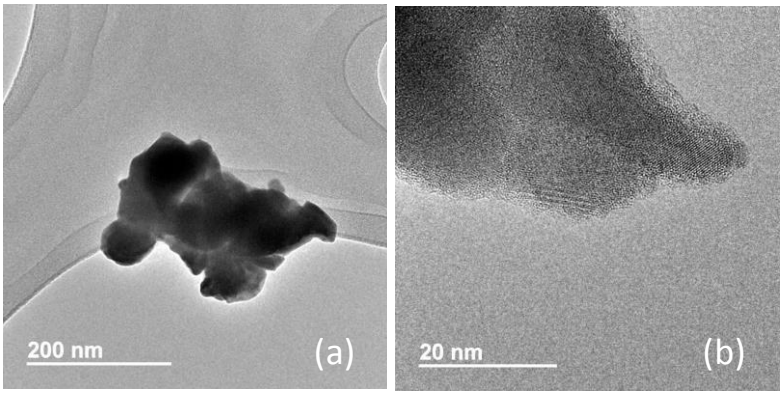

Fig 3.9: TEM image of Bi_2O_3 with PIBSA at (a) 200 nm scale (b) 20nm scale

Fig 3.9 shows the TEM image of Bi_2O_3 stabilized with PIBSA at different resolutions. Fig 3.9(a) shows that the Bi_2O_3 agglomerate has diameter in the range of ~200nm. Fig 3.9(b) shows that the crystallite size of Bi_2O_3 is in the range of 10-20nm.

Dynamic Light Scattering (DLS): Stock solution of Bi_2O_3 nanoparticles was prepared as shown in Tbale 3.11. The solution were diluted 5 times to make final nanoparticle concentration of 2mg/mL for DLS analysis.

Table 3.11: Stock solution for DLS analysis of Bi_2O_3 nanoparticles

Stabilizer	Bi_2O_3, mg/mL	Stabilizer, mg/mL	MON to Stabilizer ratio
TOFA	10	100	1:10
PIBSA	10	100	1:10
LABSA	10	100	1:10

In the case of Bi_2O_3 stabilized with TOFA the average hydrodynamic diameter of 95.5% particle is 462.5 nm and 4.5% nanoparticles is 5094 nm and in case of Bi_2O_3 stabilized with PIBSA the average hydrodynamic diameter of 98.8% particle is 234.4 nm.

Table 3.12: Average diameter of Bi_2O_3 nanoparticles with different stabilizers

Stabilizer	Peak 1		Peak 2		Peak 3		Remarks
	Avg Dia, nm	% Intensity	Avg Dia, nm	% Intensity	Avg Dia, nm	% Intensity	
LABSA	623.8	100	0	0	0	0	Bigger particles
PIBSA	234.4	98.8	5246	0.8	52.13	0.4	Some agglomeration
TOFA	462.5	95.5	5094	4.5	0	0	Significant agglomeration

In the case of Bi_2O_3 stabilized with LABSA the average hydrodynamic diameter of all 100% particle is 623.8 nm which is significantly bigger than PIBSA & TOFA stabilized nanoparticles. In case of Bi_2O_3 PIBSA has stabilized majority of nanoparticles with 234 nm diameter which is smaller among all three stabilizers.

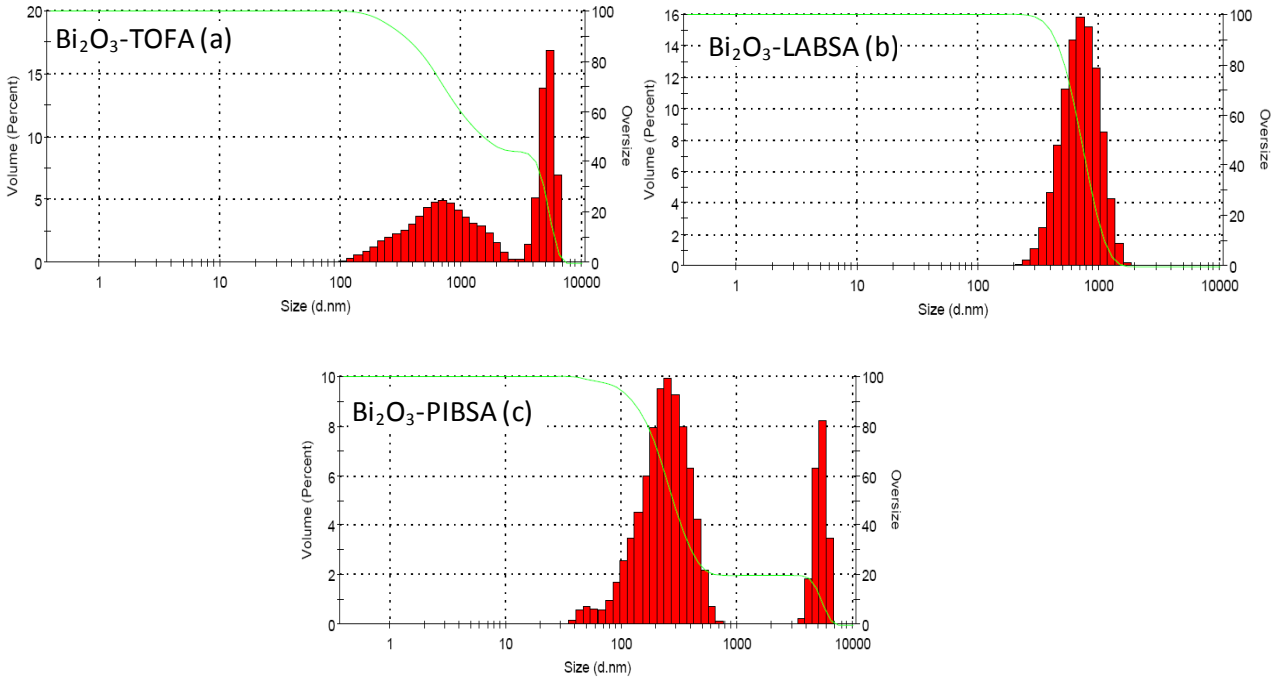

Fig 3.8: DLS images of Bi_2O_3 with (a) TOFA (b) LABSA (c) PIBSA

5.0 CONCLUSION

- Metal oxide nanoparticles of Magnesium, Cerium and Bismuth were synthesized by co-precipitation method. These nanopartcile were dispersed in toluene with the help of various stabilizers such as LABSA, PIBSA, TOFA and Alphox.

- CeO_2 nanoparticles were prepared by co-precipitation method using Cerium Nitrate and sodium hydroxide. TEM images shows that the nanoparticle are uniformly distributed having average size of agglomerated CeO_2 in the range of 40-50nm & crystallite size of CeO_2 is in the range of 5-10 nm. DLS graph shows that CeO_2 nanoparticles stabilized with LABSA have lowest average hydrodynamic diameter of 167.6 nm.

- MgO nanoparticles were prepared by co-precipitation method using Magnesium Chloride and Ammonium hydroxide. DLS graph shows that MgO stabilized with TOFA has the lowest average hydrodynamic diameter of 245nm. The average hydrodynamic diametrs of MgO stabilized with LABSA and PIBSA were 525.9nm and 323.4nm respetively.

- Bi_2O_3 nanoparticles were prepared by co-precipitation method using Bismuth Nitrate and Ammonia. DLS graph shows that Bi_2O_3 stabilized with PIBSA has stabilized majority of nanoparticles with averagen hydrodynamic diameter of 234nm which is smaller than Bi_2O_3 stabilized with TOFA (462.5 nm) and LABSA (623.8 nm).

- These stable dispersion of nanoparticles will be tested as additives in various refinery applications which is not the scope in this study.

REFERENCES

1. Wolf E. L and Medikonda M. (2012), 'Understanding the Nanotechnology Revolution';Wiley: New York.
2. Kong X., & Ohadi, M. (2010). 'Applications of Micro and Nano Technologies in the Oil and Gas Industry - Overview of the Recent Progress'. Society of Petroleum Engineers.
3. Ying J.Y, and Sun T. (1997). Research Needs Assessment on Nano-structured Catalysts, Journal of Electroceramics, Vol 1, No.3, pp.219-238.
4. Theodore L. Kunz R. G (2005). 'Nanotechnology: Environmental Implications and Solutions'; Wiley: New York.
5. Haruta M., Yamada N., Kobayashi T., Iijima S (1989). 'Gold catalysts prepared by coprecipitation for low-temperature oxidation of hydrogen and of carbon monoxide'. J. Catal., Vol 115, No. 2, pp. 301–309.
6. Palomba S., Novotny L., Palmer R (2008). 'Blue-shifted plasmon resonance of individual size-selected gold nanoparticles'. Opt. Commun., Vol 281,No. 3,pp. 480–483.
7. Poinern G. E. J., Shackleton R., Mamun S.I., Fawcett D (2011). 'Significance of novel bioinorganic anodic aluminum oxide nano scaffolds for promoting cellular response.' Nanotechnol. Sci. Appl. Vol 11, No. 4, pp.11–24.
8. Poinern G. E. J., Le X. T., Shan S., Ellis T.,Fenwick, S., Edwards J., Fawcett D. (2011).'Ultrasonic synthetic technique to manufacture a pHEMA nanopolymeric-based vaccine against the H6N2 avian influenza virus: a preliminary investigation'. Int. J. Nanomed. Vol 11, No. 6, pp. 2167–2174.
9. Bruchez M., Moronne M., Gin P., Weiss S., Alivisatos A. P (1998). 'Semiconductor nanocrystals as fluorescent biological labels'. Science. Vol 281, No. 5385, pp.2013–2016.
10. Murray C.B., Norris D.J., Bawendi M.G.(1993). 'Synthesis and characterization of nearly monodisperse CdE (E = sulfur, selenium, tellurium) semiconductor nanocrystallites.' J. Am. Chem. Soc., Vol 115, No. 19, pp. 8706–8715.
11. Bottini M., Mustelin T. (2007) Carbon materials: nanosynthesis by candlelight. Nat. Nanotechnol, Vol 2, No .10, pp.599–600.
12. Ijima S. (1991). Helical microtubules of graphitic carbon. Nature, Vol 354, No. 6348, pp.56 58.
13. Kolthoff I M (1932). Theory of co-precipitation. The formation and properties of crystalline precipitates. J Phys. Chem, Vol 36, No. 3, pp. 860–881.
14. Turkevich J., Stevenson P C., Hillier J (1951). 'A study of the nucleation and growth processes in the synthesis of colloidal gold. Discuss.' Faraday Soc, Vol 11,pp. 55–75.
15. Znaidi L., Touam T.,Vrel D., Souded N., Ben Yahia S., Brinza O., Fischer A., Boudrioua A.(2012). ZnO thin films synthesized by sol-gel process for photonic applications. Acta Phys. Pol. A, vol 121, No 1, pp.165–168.

16. Malik M.A, Wani M.Y, Hashim M.A (2012). 'Micro emulsion method: A novel route to synthesize organic and inorganic nanomaterials.' Arabian Journal of Chemistry. Volume 5, Issue 4, pp- 397–417.

17. Book "A laboratory course in nanoscience and nanotechnology", Dr. Gérrard Eddy Jai Poinern, CRC press, 2014.

18. Bootz A,Vogel V, Schubert D, Kreuter J.(2004). Comparison of SEM, DLS and analytical ultracentrifugation for the sizing of polybutyl cyanoacrylate nano particles. European Journal of Pharmaceutics and Biopharmaceutics. Volume 57, Issue 2, March 2004, pp.369–375.

19. Ingham B (2015). 'X-Ray scattering characterization of nanoparticles'. Crystallography Reviews, Vol 21, No.4, pp. 229-303.

20. Jans H, Liu X, Austin L, Maes G and Huo Q (2009). Anal Chem Vol 81, Issue 22, pp. 9425–9432.

21. Aragon SR, Pecora R (1976). 'Theory of dynamic light scattering from polydisperse systems'. The Journal of Chemical Physics, Vol 64, pp.2395.

22. International Journal of Environmental Science and Development 2013, Vol. 4(3)

23. Arabian Journal of Chemistry 2015, Vol 8, 279-284.

24. Journal of Scientific and Industrial Research 2014; Vol 73,pp. 87-90.

25. Kumar S.S., Venkateswarlu P., Rao V.R. et al (2013). 'Synthesis, characterization and optical properties of zinc oxide nanoparticles'. Int Nano Let Vol 3, No.30

26. N. Srinivasan, C. Rangasami, J.C. Kannan, "Synthesis structure and optical properties of zinc oxide nanoparticles" International Journal of Applied Engineering Research, Vol. 10 No.67 (2015).

27. Phyu Phyu Win, Myint Sanda Win, Nanotechnology Research Department, Metallurgical Research and Development Centre, Ministry of Science and Technology, Myanmar.

28. Phiwdang K, Suphankij S, Mekprasart W, Pecharapa W (2013). 'Synthesis of CuO nanoparticles by precipitation method using different precursors'. Energy Procedia , Vol 34, pp.740-745.

29. I. Z. Luna, et al (2015). Preparation and Characterization of Copper Oxide Nanoparticles Synthesized via Chemical Precipitation Method, Volume 2, e1409.

30. Saif S, Tahir A, Asim T and Chen Y. (2016). Plant mediated green synthesis of CuO Nanoparticles: Comparison of toxicity of engineered and plant mediated CuO nanoparticles. Nanomaterials, Vol 6 pp.205.

31. R.K. Jha, Pasricha R., Ravi V (2005).Synthesis of bismuth oxide using bismuth nitrate and urea. Ceramics International. Vol 31, No.3, pp. 495-497.

32. Masui T, Hirai H, Imanaka N, Adachi G (2002). Synthesis of cerium oxide nanoparticles by hydrothermal crystallization with citric acid. Journal of materials science letters,Vol 21, pp. 489 – 491

33. Patil M.M, Deshpande V.V, Dhage S.R, Ravi V (2005). Materials Letter.Vol 59, pp. 2523-2525

34. Chin H.S., Cheong K.Y. & Razak K.A (2010). Review on oxides of antimony oxide nanoparticles. Synthesis, properties and applications. J Mater Sci, Vol 45, pp. 5993-6008.

35. Zhang Z, Guo L, Wang W (2001). Synthesis and characterization of antimony oxide nanoparticles. Vol 16, No. 3, pp. 803-805.

36. Journal of Alloys and Compounds 509 (2011) 7881-7885

37. Stengl V, Bakardjieva M, Marikova P, Bezdicka J (2003).'Magnesium oxide nanoparticles prepared by ultrasound enhanced hydrolysis of Mg alkoxides'. Material letters, Vol 57, pp.3998-4003

38. J Kavitha P, Ramesh R, Rajan M.R, Stella C (2015). Synthesis and Characterization of Cerium Oxide Nanoparticles by Using Rapid Precipitation Method. Paripex- Indian Journal of Research.Vol 4, No. 12, pp. 91-93

39. Jasmin K J and Samson AN (2011). Synthesis of CeO2 nanoparticles by chemical precipitation and the effect of a surfactant on the distribution of particle sizes. J of Ceramic Processing Research. Vol 12, No 1, pp. 74-79.

40. Benmouhoub C, Kadri A, Benbrahim N, Hadji S (2009). 'Synthesis and Characterization of Cerium Oxide (CeO2) Nanoparticles'. Materials Science Forum, Vol. 609, pp. 189-194.

41. Ranjbar M, Yousefi M , Lahooti M, Malekzadeh A.(2012) 'Preparation and Characterization of Tetragonal Zirconium Oxide Nanocrystals from Isophthalic Acid-Zirconium(IV) Nanocomposite As a New Precursor'.Int J Nanoscience. Vol 8, No. 4 , pp. 191-196.

42. Tyagi B , Sidhpuria K, Shaik B, and Vir Jasra R (2006). Synthesis of nanocrystalline zirconia using sol gel and precipitation techniques. Ind Eng Chem Res.,Vol 45, No. 25, pp. 8643–8650.

43. International Journal of Chemical, Molecular, Nuclear, Materials and Metallurgical Engineering 2012.Vol 6, No.4

44. Mahshad A, Rashidi, Morad A, Bakhtiari, Iida (2014). Preparation of High Surface Area ZrO2 Nanoparticles. Iran J Chem Eng .Vol 33, No 2, pp.47-53.

45. Parviz D, Kazemeini M, Rashidi A, Jozani J (2009). Synthesis and characterization of MoO3 nanostructures by solution combustion method employing morphology and size control. J Nanopart Res,Vol 12, pp.1509-1521.

46. Chem. Mater. 2007, Vol.19, pp 1103-1110

47. Griffin, William C. (1954). Calculation of HLB values of non-ionic surfactants. Journal of the Society of Cosmetic Chemists, vol 5, no 4, pp. 249-56

48. Davies JT (1957). 'A quantitative kinetic theory of emulsion type.I. Physical chemistry of the emulsifying agent'. Proceedings of the International Congress of Surface Activity, pp.426-38